



HAL
open science

Study of the behavior of copper species in presence of pollutants in steam generator flow-restricted areas

Thibault Vital, Marion Roy, Dominique You

► To cite this version:

Thibault Vital, Marion Roy, Dominique You. Study of the behavior of copper species in presence of pollutants in steam generator flow-restricted areas. Fontevraud 10 - International Symposium Contribution of Materials Investigations and Operating Experience to LWRs' Safety, Performance and Reliability, SFEN, Sep 2022, Avignon, France. cea-03938683

HAL Id: cea-03938683

<https://cea.hal.science/cea-03938683>

Submitted on 13 Jan 2023

HAL is a multi-disciplinary open access archive for the deposit and dissemination of scientific research documents, whether they are published or not. The documents may come from teaching and research institutions in France or abroad, or from public or private research centers.

L'archive ouverte pluridisciplinaire **HAL**, est destinée au dépôt et à la diffusion de documents scientifiques de niveau recherche, publiés ou non, émanant des établissements d'enseignement et de recherche français ou étrangers, des laboratoires publics ou privés.

Study of the behavior of copper species in presence of pollutants in steam generator flow-restricted areas

T. Vital^{1*}, M. Roy¹, D. You¹

¹Université Paris-Saclay, CEA, Service d'Etude du Comportement des Radionucléides, 91191, Gif-sur-Yvette, France

*Corresponding Author, E-mail: thibault.vital@cea.fr

In a steam generator (SG) of a Pressurized Water Reactor (PWR), the hideout process can occur in flow-restricted areas. Non-volatile polluting species tend to accumulate in these regions due to boiling. Their concentrations can reach up to several orders of magnitude [1] above those encountered in the chemical conditioning yielding extreme pH values. Such pollutants include various metallic elements like iron, nickel, sodium, aluminum or copper, and other ions like sulfates, chlorides or phosphates. Some authors have already discussed the behavior of solid copper species in presence of phosphate under secondary circuit thermochemical conditions. Turner *et al.* [2] showed how sodium phosphate lead to a consolidation of a magnetite-copper sludge already formed with few information on which phases were observed, and Ziemniak *et al.* [3] and Palmer [4] had a major focus on the dissolved species rather than the solids. This study is a step towards a more complete description of the flow-restricted areas, including the interaction of copper and copper oxides with other species present in the secondary circuit. The objective was to identify the stable solid copper-containing species under the thermochemical conditions encountered in SG flow-restricted areas.

Keywords: copper oxides, phosphate, sodium, magnetite, reducing media, oxidizing media, PWR

1. Introduction

In power plants equipped with copper-containing condensers, metallic copper is often found inside steam generator (SG) deposits. It can account for up to 50 % by weight (w%) of the deposits [5], but is generally found around 5 w% [5], [6], the rest of it being mostly magnetite, Fe_3O_4 (> 85 w%). Those deposits are usually resulting from flow-restricted areas where a hideout phenomenon has concentrated non-volatile polluting species such as metal cations, sulfates, chlorides, or phosphates. The latter were originally used as the main chemical conditioning during the 1970s, but were abandoned in the late 1970s/early 1980s because of the difficulty to maintain the right chemical conditions in the steam generator [7]. Indeed, sodium and phosphate would locally behave differently than in the bulk, which would displace the Na/PO_4 ratio and locally shift the pH to values out of the optimal range, leading to catastrophic stress corrosion cracking or wastage of the tubing [7]. This phenomenon has been observed for many years, but the precipitates have barely been studied and the precise reasons why the chemistry is so hard to maintain with a phosphate environment are still to be determined. Interactions of copper with such environment have already been discussed extensively in the literature [2]–[6], [8]–[14], but no emphasis has been made on the redox conditions and their influence on the speciation of copper and phosphate precipitates in the steam generator thermochemical conditions. Indeed, the redox potential of the secondary circuit is usually reducing to minimize the oxidation of the metallic parts that are exposed to the fluid. Different approaches to this matter have been studied, such as the use of hydrazine as a reducing agent at high temperatures. Voluntary oxygen inlets have been implemented in several German power plants [15]–[17], because the resulting hematite deposit on the preheaters is more resistant to flow-accelerated-corrosion (FAC) than the standard magnetite deposit. Leaks from the tertiary circuit into the secondary circuit are a rare phenomenon, but they should be taken into account, especially in older power plants equipped with condensers in copper containing alloys, which can leak because of poor welding/design combined with corrosion (especially in seawater environments). However, to our knowledge, there are no studies about the behavior of copper in case a short oxygen inlet happens in SG conditions.

The goal of this study is to identify the thermodynamically stable phases under nominal and aerated conditions with a concentrated sodium phosphate environment. Precipitates containing metal-phosphate phases are under scrutiny, as well as the solid copper species oxidation number.

Thus, in this work, three experiments were conducted, two with reducing conditions, and one with aerated conditions. Three different simple solid copper species were used for the tests, metallic copper $\text{Cu}_{(s)}$, cuprous oxide $\text{Cu}_2\text{O}_{(s)}$ and cupric oxide $\text{CuO}_{(s)}$. Magnetite $\text{Fe}_3\text{O}_4_{(s)}$ was added to one of the reducing conditions tests because of its overall presence inside SG deposits in order to see if a reaction with copper and/or sodium phosphates would occur. In the magnetite-containing test, the Fe/Cu molar ratio was $[\text{Fe} : \text{Cu}] = [2.3 : 0.7]$, which corresponds to one of the possible ratios in order to obtain the $\text{Cu}_x\text{Fe}_{3-x}\text{O}_4$ ($0 < x \leq 1$) cuprospinel [18]. The appearance of a cuprospinel phase was considered because Hermansson's [13] work with solubilities and theoretical Pourbaix diagrams in the Fe-Cu-O-H system lead to the conclusion that this phase would likely appear in the SG physico-chemical conditions.

2. Materials and methods

The tests were performed with a pressurized equipment in stainless steel able to withstand temperature and pressure conditions up to 350 °C and 150 bar. The pressurized equipment, with a 1 L maximum capacity, was thoroughly washed with deionized water and a [acetone : ethanol] = [1 : 1] mix.

In all experiments, powders of the three simple solid copper species, $\text{Cu}_{(s)}$, $\text{Cu}_2\text{O}_{(s)}$ and $\text{CuO}_{(s)}$ were contained separately inside metallic copper tubes within the reactor. For the two experiments without Fe_3O_4 , an equivalent volume of each powder was introduced in the copper tubes. For the last experiment, a total mass of 10 g of powder per tube is weighed, with the molar ratio $[\text{Fe} : \text{Cu}] = [2.3 : 0.7]$. Each tube had a 50 mL capacity and was left open so that its content could interact with the environment. Oxide traces on the tubes were previously removed by mechanical polishing and chemical rinsing with a 0.1 w% HNO_3 aqueous solution. A concentrated phosphate solution was prepared ($[\text{PO}_4^{3-}] = 0.5 \text{ mol kg}^{-1} = 49.49 \text{ g kg}^{-1}$) with a $\text{Na}^+/\text{PO}_4^{3-}$ ratio [3] of 2.4 using sodium phosphate monobasic NaH_2PO_4 , sodium phosphate dibasic Na_2HPO_4 and sodium phosphate tribasic dodecahydrate $\text{Na}_3\text{PO}_4 \cdot 12\text{H}_2\text{O}$. The pH of the solution was measured at $\text{pH}_{25^\circ\text{C}} = 11$. This solution was introduced in the reactor and in the tubes up to half of the total volume. The equipment was hermetically closed, and the chosen gas was injected. Pure dihydrogen gas was used to simulate reducing conditions with concentrations respectively of $[\text{H}_2] = 35 \text{ cm}^3 \text{ kg}^{-1}$ ($P_{\text{H}_2} = 2.1 \text{ bar}$) for the experiment with copper powders only and $[\text{H}_2] = 79 \text{ cm}^3 \text{ kg}^{-1}$ ($P_{\text{H}_2} = 4.5 \text{ bar}$) for the one with copper powders and magnetite. Synthetic air with a $20.9 \pm 1 \%$ by volume (vol%) of O_2 was used for the aerated conditions to reach a concentration of $[\text{O}_2] = 17 \text{ mg kg}^{-1}$ ($P_{\text{Total}} = 2.2 \text{ bar}$, $P_{\text{O}_2} = 0.46 \text{ bar}$).

A temperature of 250 °C was imposed using a furnace, with a temperature ramp of 100 °C h^{-1} . Because of the two-phase environment applied, the total pressure adjusts itself to the water vapor pressure, equal to 40 bar for this specific temperature. The pressure and temperature were regularly monitored, and both parameters were measured respectively at $248 \pm 3 \text{ }^\circ\text{C}$ and $38 \pm 2 \text{ bar}$ over the duration of the experiments. The temperature was maintained during 312 h for the reducing conditions with the copper powders only, 720 h for the reducing conditions with Fe_3O_4 and 408 h for the aerated conditions. Upon opening the reactor the powders were collected and dried overnight in an oven at 85 °C, then placed in a desiccant cabinet.

The powders used in these experiments were high-purity solids from GoodFellow for the metallic copper (99 % stated purity), Merck for the cuprous oxide (> 96 % stated purity), Aldrich for the cupric oxide (> 99.99 % stated purity), Alfa Aesar for the magnetite powder (97 % stated purity) and VWR for the sodium phosphate monobasic, dibasic and tribasic (respectively 100 %, > 99 % and 100 % stated purity). Inductively coupled plasma mass spectrometry (ICP-MS) of the initial copper powders dissolved into an acidic solution revealed no detectable elemental impurities besides nickel and lead, both under their quantification limits (400 ng kg^{-1} and 10 ng kg^{-1} respectively). The main impurity found in the magnetite powder was silicon (0.24 w%) using a UV-Vis method. ICP-MS analysis on the magnetite powder also revealed several trace impurities, like aluminum, chromium, manganese, cobalt, nickel, gallium and barium. All chemicals were used without further purification. Solutions were prepared using highly pure distilled water which was vacuum degassed for 4 h. In this work, when referring to Cu, Cu_2O , CuO or Fe_3O_4 powders, the term is referring to the composition of the powder prior to its introduction in the reactor. The Cu powder had a distinctive metallic copper color, the Cu_2O powder was purple-red, and the CuO and Fe_3O_4 powders were a deep black (see Figure 1).

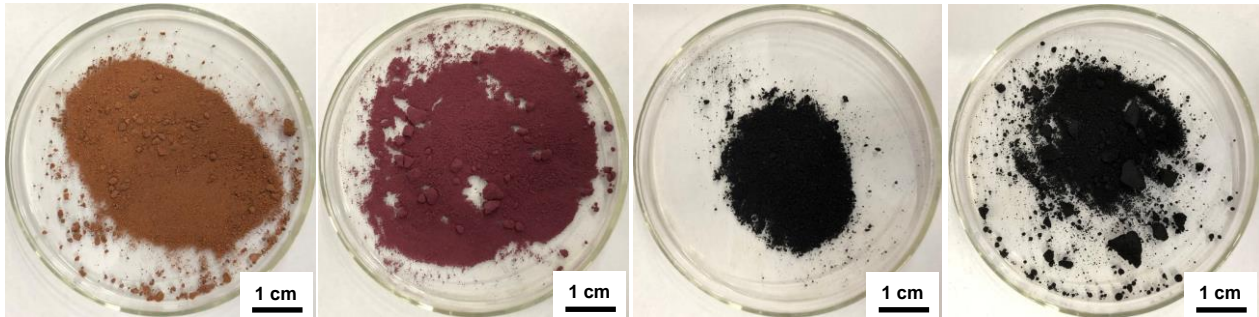


Figure 1 : Initial powders respectively from left to right Cu, Cu₂O, CuO and Fe₃O₄

The initial powders and the ones collected after each experiment were observed using a scanning electron microscope (SEM) through backscattered electrons (BSE) imaging, and analyzed through energy-dispersive X-ray spectroscopy (EDS) and X-ray diffraction (XRD). For the latter, phase identification was carried out with a PANALYTICAL X'Pert3 Powder diffractometer equipped with a copper anode tube of K_α radiation ($\lambda = 1.54 \text{ \AA}$) and operating at a voltage of 45 kV and a current of 40 mA. The detection limit for the XRD under this set of parameters was estimated at 1 vol%. The reference datasheets for peak indexation were taken from the International Centre for Diffraction Data (ICDD) database, and are given for each species. The threshold limits indicated for each reference datasheet are the intensity limits under which peaks are not displayed on the diffractograms for legibility purposes.

3. Results and discussion

3.1 Behavior of copper species under reducing conditions

3.1.1 Behavior of Cu, Cu₂O and CuO in a Na-PO₄ environment

In the experiment with copper powders only, it appeared from a macroscopic scale that the powders recovered and dried after the experiment did not change from the original powders. SEM observations in Figure 2 confirmed that no significant changes in microscopic morphology were observed on metallic copper powder and Cu₂O powder. The Cu dendrites agglomerated but no unordinary growths were noted, and for the Cu₂O the crystal edges sharpened. However, observations of the CuO powder showed the formation of large crystals with sharp edges and a size of a few micrometers, similar to those found in the Cu₂O powder. EDS analysis of the crystals in the CuO powder confirmed that they had a stoichiometric elemental composition close to Cu₂O (1.4 to 1.9).

The XRD diagrams of the powders recovered after the experiments are shown in Figure 3. Their comparison with those of the initial powders showed that the Cu powder after the experiment had no crystalline impurities. However, it was also observable in Figure 3 b) and c) that both Cu₂O and CuO powders contained new phases. The Cu₂O powder had traces (< 1 % for the largest peak intensity) of metallic copper, and the CuO powder had 100 % intensity peaks for both CuO and Cu₂O.

In the Cu₂O powder XRD diagram, the majority of the observable peaks corresponds to Cu₂O. Since metallic Cu peaks can be picked out, at least 1 vol% of Cu₂O has been reduced into Cu. This is a very small amount, which means there was a limitation of the reaction. This limitation can be due to the slow diffusion of H₂ through Cu₂O, to the slow reduction kinetics of Cu₂O into Cu [19] or to the H₂ running out since the initial amount introduced was not renewed during the experiment.

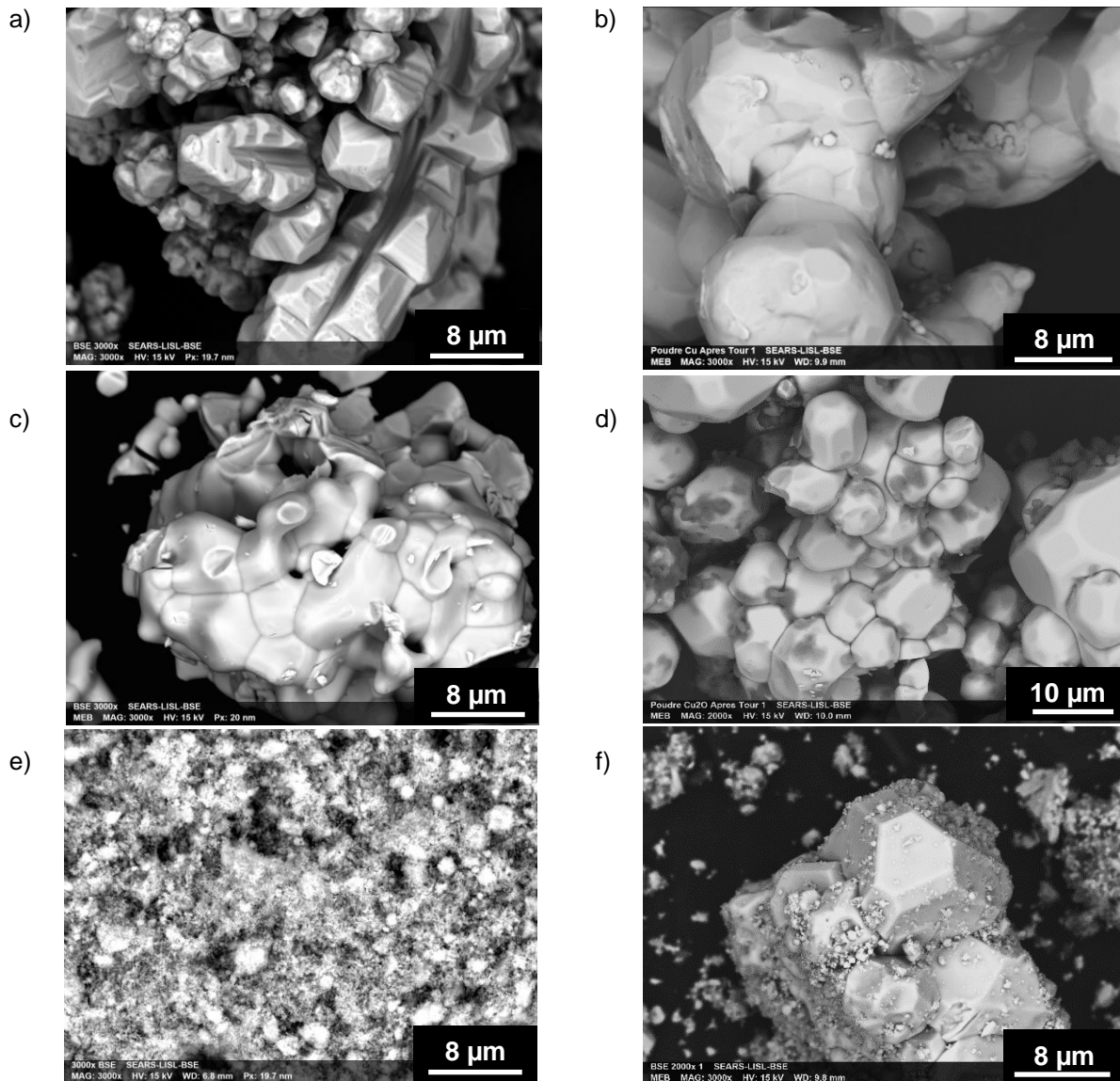
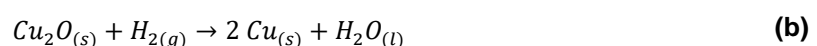
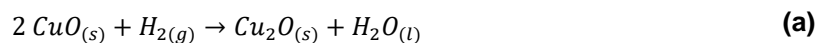


Figure 2 : Morphology of the powders observed with a SEM through BSE imaging before (a, c, e) and after (b, d, f) exposure at 250 °C with $[H_2] = 35 \text{ cm}^3 \text{ kg}^{-1}$. a) and b) are images from the Cu powder, c) and d) from the Cu_2O powder, e) and f) from the CuO powder

CuO XRD analysis did not show the formation of metallic copper. This is coherent with thermodynamic stability, because Cu^0 and Cu^{II} species cannot coexist in a stable state : Ellingham [20] and Pourbaix [21], [22] diagrams for copper systematically have a band of one or more Cu^{I} species separating Cu^0 and Cu^{II} species. This result is confirmed by Kim *et al.* [19], which show that CuO is totally reduced into Cu_2O (equilibrium (a) between CuO and Cu_2O maintains the partial pressure of H_2 at a certain value) before Cu_2O is reduced into metallic copper (equilibrium (b) maintains the partial pressure of H_2 at another value).



In the tested conditions, it was observed that CuO reduces into Cu_2O , Cu_2O reduces into Cu, and Cu is stable. It confirms that the (a) and (b) equilibria are correct. From a thermodynamic standpoint, it implies that metallic copper is the stable phase under these conditions. This conclusion is coherent with the reducing environment applied at the start of this experiment.

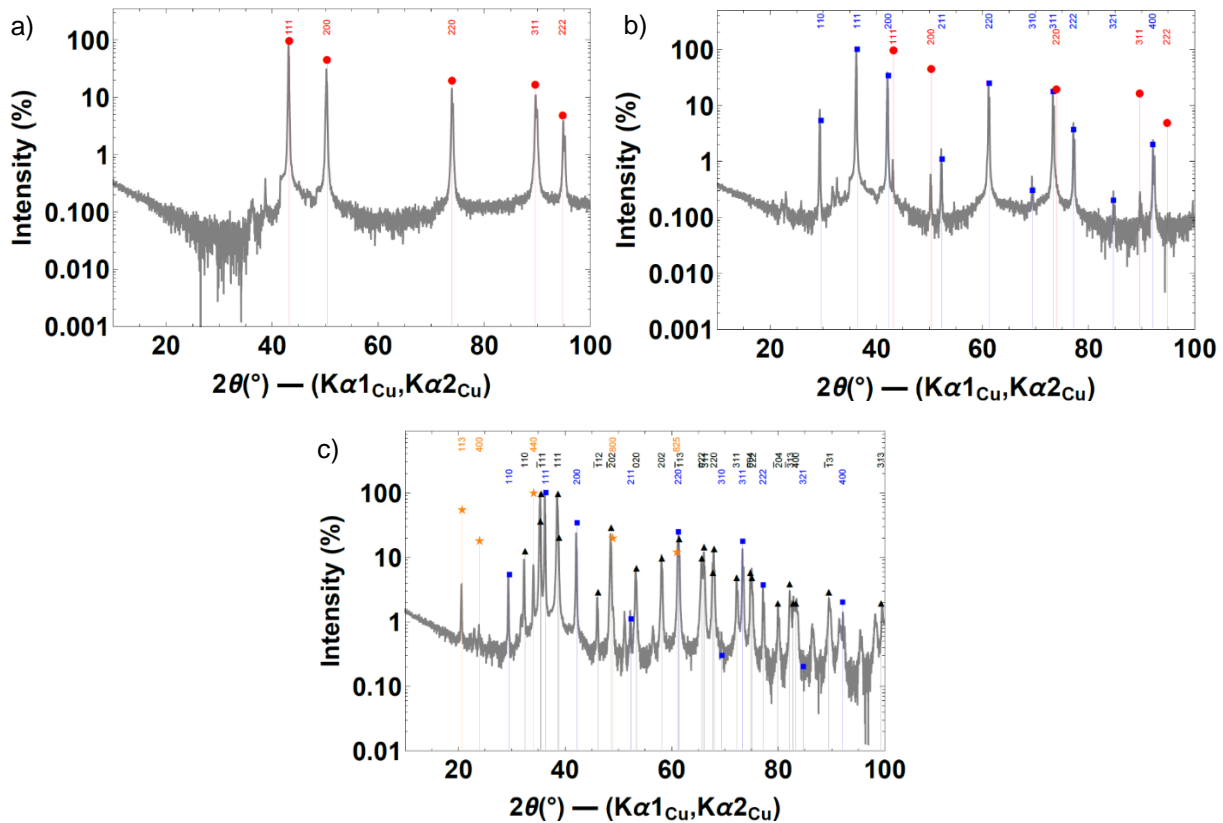


Figure 3 : XRD diagrams in Log scale for the powders after exposure at 250 °C with $[H_2] = 35 \text{ cm}^3 \text{ kg}^{-1}$, a) for Cu powder, b) for Cu_2O powder, c) for CuO powder. ● Cu reference peaks (00-004-0836, 1 % threshold), ■ Cu_2O reference peaks (01-071-3645, 1 % threshold), ▲ CuO reference peaks (00-048-1548, 1 % threshold), ★ Na_3PO_4 reference peaks (00-031-1323, 10 % threshold)

3.1.2 Behavior of Cu, Cu_2O and CuO in presence of Fe_3O_4 in a Na- PO_4 environment

In the proportions introduced for this test (molar ratio $[\text{Fe} : \text{Cu}] = [2.3 : 0.7]$), magnetite was in much larger quantity than the copper species. This means that the mixed powders introduced in the reactor prior to the experiment were all black, which also was the appearance of the powders recovered after the experiment, and no changes on the macroscopic scale were noted.

SEM observations are presented in Figure 4. Similar morphology was observed on all samples. Bright, rounded structures of about ten micrometers in length were observed, which EDS analysis revealed were mostly composed of copper. Small, noticeably darker octahedron crystals were visible with a size of a micrometer or less, and EDS analysis showed that they were primarily composed of iron and oxygen with a stoichiometry close to the one of Fe_3O_4 (molar ratio $[\text{Fe} : \text{O}] = [2.8 : 4]$) or Fe_2O_3 (molar ratio $[\text{Fe} : \text{O}] = [1.7 : 3]$). The long dark crystals observed contained the elements Na, Fe, P and O, and corresponded to a phase of iron, phosphate and sodium.

Imaging and EDS analysis seemed to show that the copper oxides Cu_2O and CuO had been reduced because the measured Cu/O atomic ratios were overall greater than 2. The lowest was measured at 2.57, but most were between 3 and 5. Thus, complementary XRD analysis were conducted to identify the phases present in the samples.

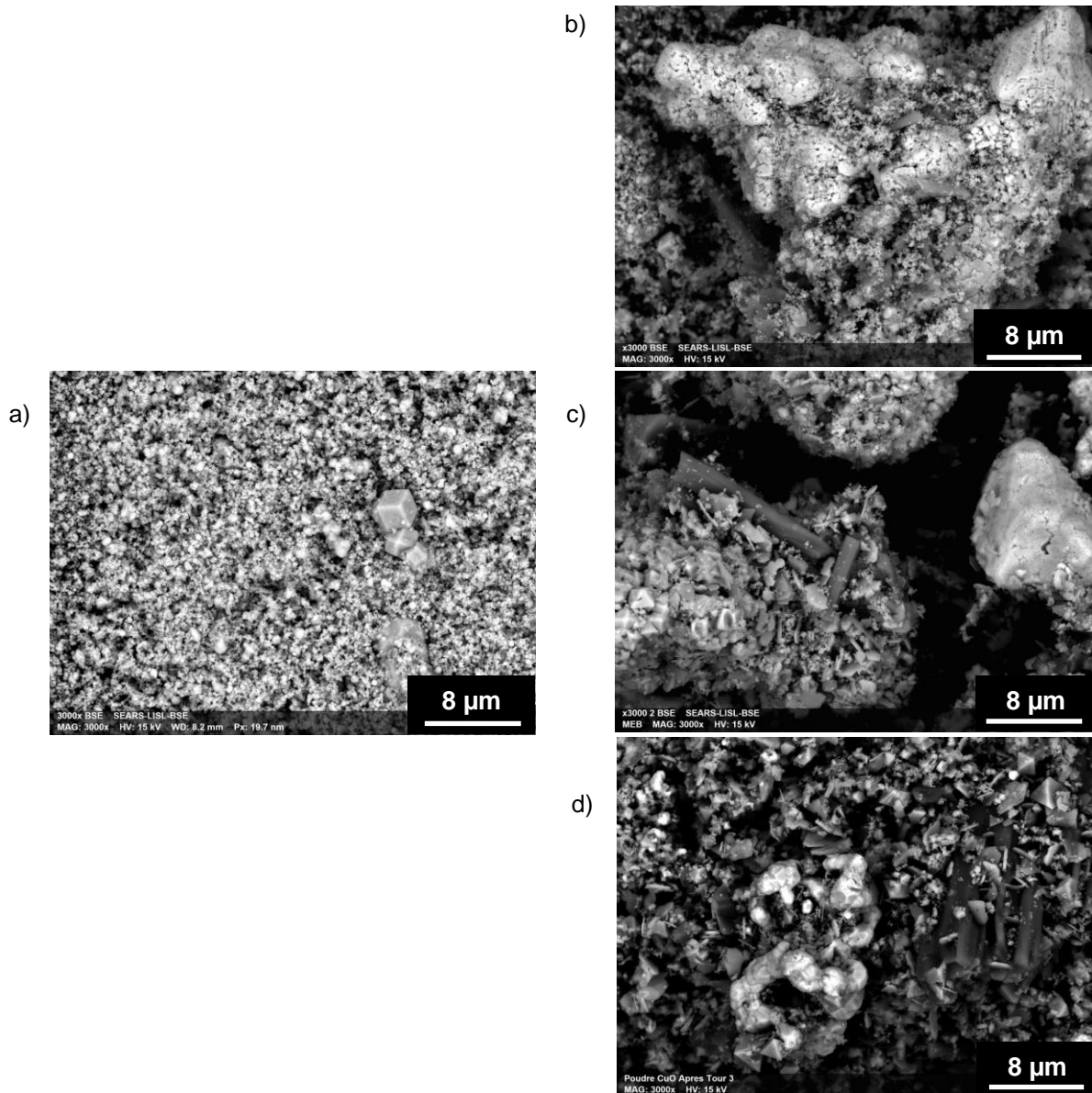


Figure 4 : Morphology of the powders observed with a SEM through BSE imaging before (a) and after (b, c, d) exposure at 250 °C with $[H_2] = 79 \text{ cm}^3 \text{ kg}^{-1}$ in presence of magnetite. a) is an image from the Fe_3O_4 powder, b) from the Cu/Fe_3O_4 powder, c) from the Cu_2O/Fe_3O_4 powder, and d) from the CuO/Fe_3O_4 powder

Spinel phases, which have a common face-centered cubic-type (FCC) crystal structure, have similar XRD diffractograms. Only a slight shift towards high 2θ and a few additional peaks with an intensity lesser than one percent (for a normalized intensity) allow for a distinction. In the case of the cuprospinel $Cu_xFe_{3-x}O_4$ ($0 < x \leq 1$) and magnetite Fe_3O_4 , the only difference is the substitution of Fe^{II} cations by Cu^{II} cations. This substitution causes weak distortions of the FCC crystal lattice (radius difference of about 5 pm), but more importantly it modifies the structure factor.

Thus, the peaks of the diffractograms of $Cu_xFe_{3-x}O_4$ and Fe_3O_4 should be shifted by a few tenths of a degree at most, which makes the exact phase more difficult to characterize. Thus, a method using an internal Ni standard calibration was applied. This process consists in adding an inert and known phase, used as a reference, to the powders analyzed. It is then possible to compare the most intense and distinct peaks from this reference's datasheet with the corresponding peaks obtained in the XRD diagrams. This calibration allows a higher precision by shifting the diagrams to match the reference perfectly.

The XRD diagrams in Log scale are shown Figure 5, and the first identifiable phase common to each of the powders was metallic copper, which is consistent with the applied reducing environment and the EDS and XRD results obtained in the test without Fe₃O₄.

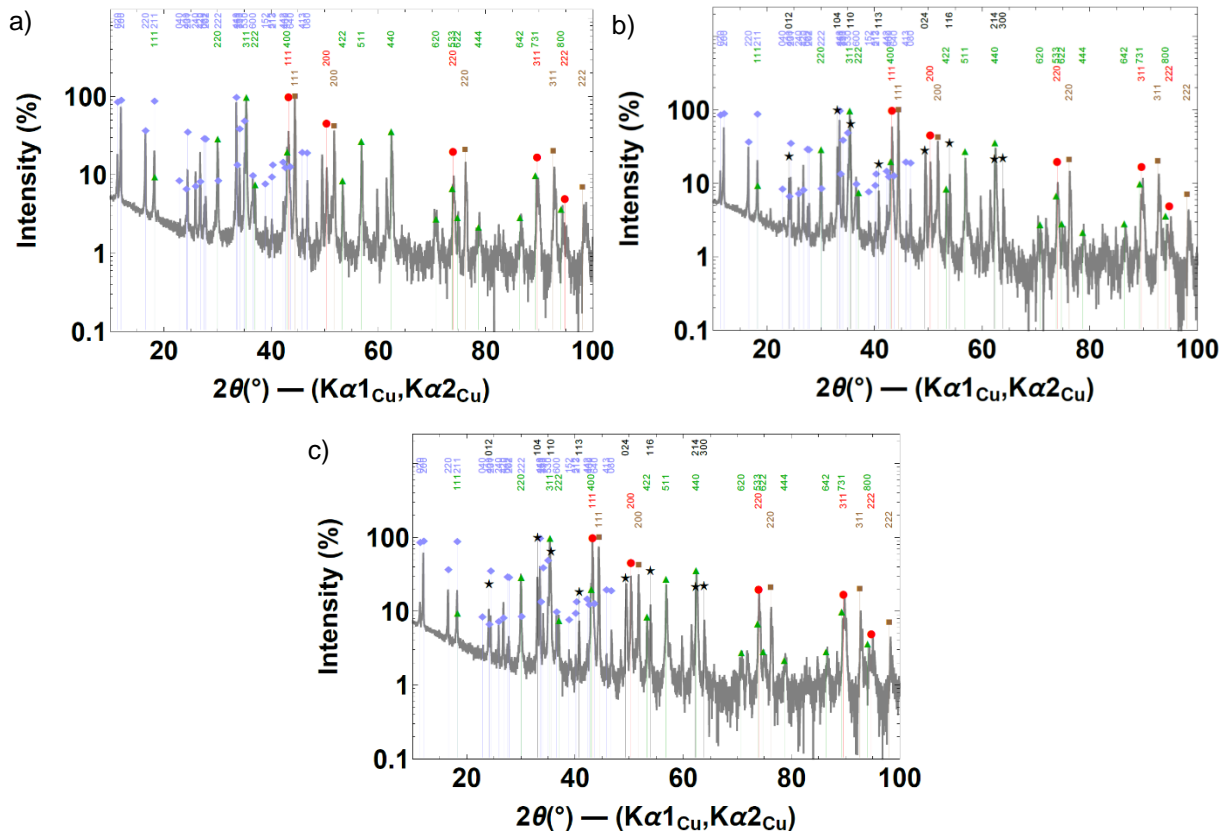
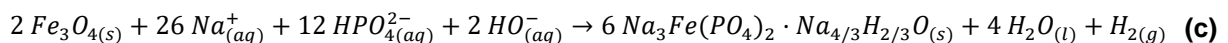


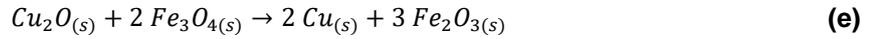
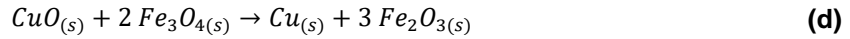
Figure 5 : XRD diagrams in Log scale for the powders with addition of Ni after exposure at 250 °C with [H₂] = 79 cm³ kg⁻¹ in presence of magnetite, a) for Cu/Fe₃O₄ powder, b) for Cu₂O/Fe₃O₄ powder, c) for CuO/Fe₃O₄ powder. ● Cu reference peaks (00-004-0836, 1 % threshold), ■ Ni reference peaks (00-004-0850, 1 % threshold), ▲ spinel (Fe₃O₄) reference peaks (01-079-0418, 1 % threshold), ◆ Na_{4.55}Fe(PO₄)₂H_{0.45}O reference peaks (00-052-1393, 5 % threshold), ★ Fe₂O₃ hematite reference peaks (01-089-0596, 10 % threshold)

A mixed Na-Fe-PO₄ phase was also observed in all the powders, sodium iron hydroxyphosphate (SIHP). This phase was given with the formula Na_{4.55}Fe(PO₄)₂H_{0.45}O in the XRD reference database used in this work. It was obtained under very similar experimental conditions by Bridson *et al.* [23], with stoichiometric coefficients for sodium and hydrogen defined such that the phase is written Na₃Fe(PO₄)₂·Na_{2(1-x)}H_{2x}O, with x = 0.226 ± 0.025. The XRD peaks reference dataset provided by the author is obtained by calculation on a phase of SIHP with x = 0.225. However, its stoichiometry is not completely established. Indeed, Broadbent *et al.* [24], Ziemiak and Opalka [25], Quinlan *et al.* [26] and Tremaine and Xiao [27] found the stoichiometry of SIHP to be Na₃Fe(PO₄)₂·Na_{4/3}H_{2/3}O. The formation of this compound from magnetite and sodium phosphate is given by the following reaction:



The presence of hematite Fe₂O₃ was noted in the two powders which initially contained Cu₂O/Fe₃O₄ and CuO/Fe₃O₄, but not Cu/Fe₃O₄. The disappearance of copper oxides and the presence of hematite indicate that a reaction between magnetite and copper oxides has taken place to form metallic copper and hematite.

Reactions (d) and (e) for cuprous oxide and cupric oxide show the reduction of copper oxides into metallic copper and the oxidation of magnetite into hematite.



Depending on the quantity of H_2 left after the complete reduction of copper oxides into metallic copper through reactions (d) and (e) but also (a) and (b), hematite has also possibly been partially reduced because all copper oxides have been reduced already. Since there was no measurement on the concentration of H_2 in the reactor at the end of the experiment, it is not possible to conclude about the hydrogen consumption by a possible reduction of the hematite formed.

Interactions between copper oxides and magnetite/hematite have been discussed by McGarvey and Owen [28], and they arrived at the same conclusion as this work. However, their experiments differed from this one by a few factors. They did not conduct their experiments with sodium phosphate chemistry, and the maximum temperature they reached was 225°C , which is close to the fluid temperature at the entrance of the steam generator from PWR, but lower than what is found in operating SG.

A spinel phase was distinguished in the XRD diffractograms. The determination of this phase was carried out by enlarging the diffractograms on intense characteristic peaks after calibration using the internal standard, metallic Ni. The peaks observed in each powder corresponded to the crystalline planes 311 and 220 of the spinel. Four different spinel phases were tested : $\text{Cu}_{0.67}\text{Fe}_{2.33}\text{O}_4$, $\text{Cu}_{0.75}\text{Fe}_{2.25}\text{O}_4$, CuFe_2O_4 and Fe_3O_4 . The exact $\text{Cu}_{0.7}\text{Fe}_{2.3}\text{O}_4$ stoichiometry (*i.e.* Fe/Cu ratio introduced in the experiment) was not referenced in the browsed ICDD database for the analysis. Nevertheless, the available stoichiometries $\text{Cu}_{0.67}\text{Fe}_{2.33}\text{O}_4$ and $\text{Cu}_{0.75}\text{Fe}_{2.25}\text{O}_4$ were very close. The enlarged diffractograms for 2θ between 29.6° and 30.4° , and 2θ between 35.0° and 35.8° are given in Figure 6. The starting spinel phase, Fe_3O_4 , as well as the cuprospinel $\text{Cu}_{0.67}\text{Fe}_{2.33}\text{O}_4$ and $\text{Cu}_{0.75}\text{Fe}_{2.25}\text{O}_4$ seemed to correspond. Indeed, the reference peaks for these phases are separated by only 0.02° , which is within the device's margin of error and barely above the measuring step which was 0.01671° . Based on those observations, it was therefore possible that the spinel in the powders was only magnetite, only a cuprospinel, or a mix of both.

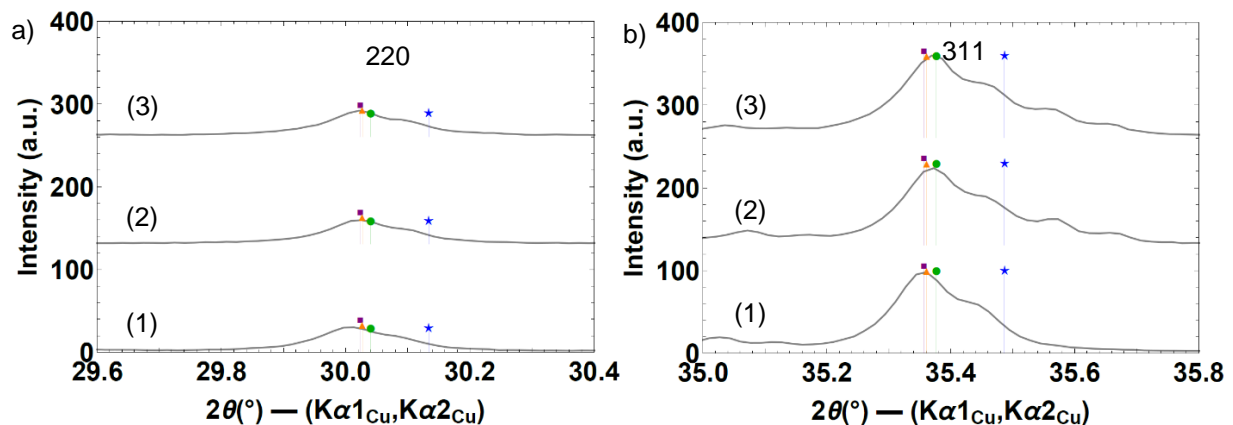


Figure 6 : XRD diagrams in linear scale for the powders with addition of Ni after exposure at 250°C with $[\text{H}_2] = 79 \text{ cm}^3 \text{ kg}^{-1}$ in presence of magnetite. Focus was made on a) the second to most intense peak of the spinel phase (2θ between 29.6° and 30.4°), and b) the most intense peak of the spinel phase (2θ between 35.0° and 35.8°). (1) $\text{Cu}/\text{Fe}_3\text{O}_4$ powder, (2) $\text{Cu}_2\text{O}/\text{Fe}_3\text{O}_4$ powder, (3) $\text{CuO}/\text{Fe}_3\text{O}_4$ powder. ● Fe_3O_4 reference peaks (01-79-0418, 1 % threshold), ■ $\text{Cu}_{0.67}\text{Fe}_{2.33}\text{O}_4$ reference peaks (01-073-2317, 1 % threshold), ▲ $\text{Cu}_{0.75}\text{Fe}_{2.25}\text{O}_4$ reference peaks (01-073-2316, 1 % threshold), ★ CuFe_2O_4 reference peaks (01-074-8585, 1 % threshold)

Further EDS characterizations and cartographies over larger portions of the samples following the XRD analysis confirmed that the spinel was largely composed of Fe and O. These results associated with the XRD results definitely ruled out the possibility that a cuprospinel had formed as Hermansson [13] claimed. While it is possible that the reaction kinetics to form this phase is so slow that a month under those conditions was not enough to obtain detectable amounts of the cuprospinel, Shishin [29] indicates that CuFe_2O_4 is a metastable phase under 544 °C. The results obtained in this study tend to corroborate the latter theory.

To conclude on the behavior of copper in presence of magnetite, the total reduction of copper oxides to metallic copper and the stability of metallic copper show that the latter is the only solid copper species thermodynamically stable under the conditions applied in this test. No cuprospinel phases were formed, but copper oxides and magnetite reacted to form metallic copper and hematite. It confirmed that copper can provide an oxidizing environment for iron species. Hematite in itself is not harmful, but the structure change from magnetite to hematite can destabilize the magnetite passivation layer [30], which reactivates the corrosion by exposing non oxidized materials.

3.2 Behavior of Cu, Cu_2O and CuO in a Na-PO_4 environment under oxidizing initial conditions

In appearance, after the test the powders looked like a mix of the original copper powders and white crystals, which were assumed to be sodium phosphate precipitates. Figure 7 shows the microscopic morphologies of each of the powders after conditioning under an oxidizing atmosphere. No significant changes in morphology were observed in the Cu_2O powder. In Cu and CuO powders, small cubic crystals similar in shape to those found in the Cu_2O powder appeared. Dark crystals observed through BSE imaging had an elemental composition of Na, P and O according to EDS analysis. More EDS analysis showed that the Cu_2O and CuO powders retained their initial elemental composition, but that the Cu powder locally had different compositions. Indeed, some small crystals had a Cu/O atomic ratio of 2. The appearance of the crystals observed in the Cu powder and their composition were compatible with a Cu_2O phase.

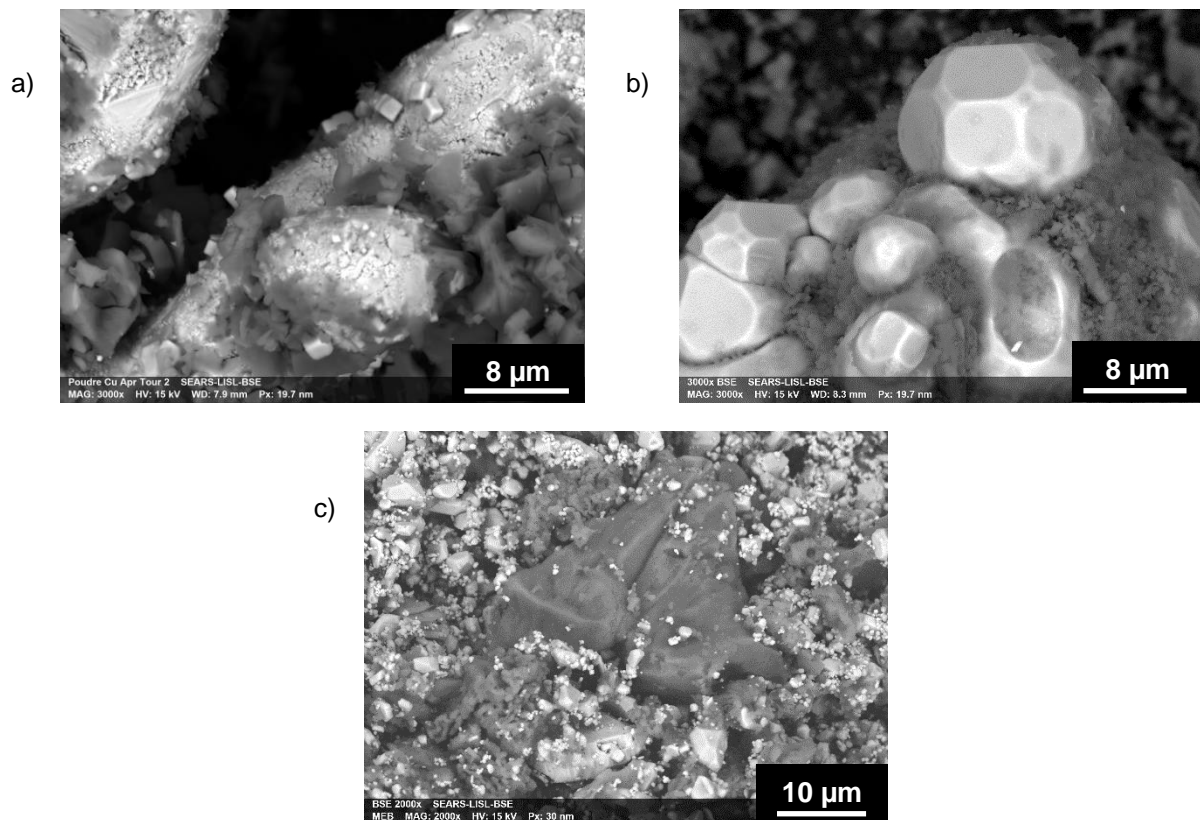


Figure 7 : Morphology of the powders observed with a SEM through BSE imaging after exposure at 250 °C with $[\text{O}_2] = 17 \text{ mg kg}^{-1}$. a) is an image from the Cu powder, b) from the Cu_2O powder, c) from the CuO powder

4. Conclusion

The stable species of copper under the thermochemical conditions encountered in steam generator flow restricted areas of a PWR were determined.

First, this work confirms that metallic copper is the stable copper-containing solid phase under aqueous nominal reducing conditions, despite the high phosphate concentration and the presence or not of magnetite, which is in agreement with field results from PWR [31], [32]. It was also observed that an oxidized copper species would rather react with magnetite and oxidize it into hematite than being directly reduced in the nominal operating conditions. This observation confirms that the presence of copper oxides inside the steam generator can lead to an oxidizing environment for magnetite [28], creating clusters of hematite.

Second, it was shown that a punctual oxygen inlet would have an influence on the composition of solid copper species, the stable species determined to be cuprous oxide. This result, combined with the previous results, would indicate that if an oxygen inlet reached a flow-restricted area, the magnetite deposits in the vicinity of copper deposits would react into hematite. Thus, it is essential to eliminate copper oxides and their source, and to avoid any introduction of these species close to less noble elements like iron.

Phosphates were shown to precipitate into sodium phosphate phases with a stoichiometry similar to the one introduced in our experiment. No copper-phosphate solid phases were observed, which means that copper does not trap the sodium phosphate chemical conditioning. However, another metal-phosphate-containing phase did precipitate. Indeed, the detection of a sodium iron hydroxyphosphate (SIHP) phase confirms that sodium and phosphate are being trapped under normal operating conditions. In that case, copper might be an indirectly aggravating factor since, under the conditions applied, its oxides Fe^{II} into Fe^{III} , the latter of which is the oxidation level present in SIHP.

The perspectives of this work are to gather the thermodynamic data of the species involved in the Cu-Fe-Na-P-O-H system and use them to lead to a better description of the behavior of polluting species inside the flow-restricted areas in the steam generator.

Acknowledgment

This work was funded by the French Alternative Energies and Atomic Energy Commission (CEA). The authors would like to thank R. Abadie and B. Duprey for their skills and assistance with the experiments, and V. Mertens for carrying out the ICP-MS analyses. Helpful discussions and advice from C. Marchand were also appreciated.

References

- [1] C. Mansour, "Spéciation des espèces soufrées dans les générateurs de vapeur des centrales nucléaires à réacteur à eau sous pression," Paris VI, Chimie ParisTech, 2007
- [2] C. W. Turner, M. E. Blimkie, and P. A. Lavoie, "Physical and Chemical Factors Affecting Sludge Consolidation," Atomic Energy of Canada Limited, Chalk River, Ontario (Canada), AECL-11674, 1997
- [3] S. E. Ziemniak, M. E. Jones, and K. E. S. Combs, "Copper(II) oxide solubility behavior in aqueous sodium phosphate solutions at elevated temperatures," *J. Solut. Chem.*, vol. 21, no. 2, pp. 179–200, 1992
- [4] D. A. Palmer, "The solubility of crystalline cupric oxide in aqueous solution from 25 °C to 400 °C," *J. Chem. Thermodyn.*, vol. 114, pp. 122–134, 2017
- [5] M. Vepsäläinen, "Deposit formation in PWR steam generators," VTT, VTT-R-00135-10, 2010
- [6] C. R. Marks, "Oxidation and reduction of copper and iron species in steam generator deposits - Effects of hydrazine, carbohydrazide and catalyzed hydrazine," INIS, Technical report INIS/34066661, 2000
- [7] A. Drexler, S. Weiss, F. Roumiguere, and J. Fandrich, "Water chemistry operation experience and steam generator maintenance measures in PWRs," presented at the AREVA NP GmbH, Erlangen (Germany), 2010
- [8] D. A. Palmer, "Solubility Measurements of Crystalline Cu_2O in Aqueous Solution as a Function of Temperature and pH," *J. Solut. Chem.*, vol. 40, no. 6, pp. 1067–1093, 2011
- [9] L. N. Var'yash, "Hydrolysis of Cu(II) at 25–350°C," *Geochem. Int.*, vol. 23, no. 1, pp. 82–92, 1985
- [10] L. N. Var'yash, "Equilibria in the Cu- Cu_2O - H_2O System at 150-450°C," *Geochem. Int.*, vol. 26, no. 10, pp. 80–90, 1989.

- [11] K. J. Powell, P. L. Brown, R. H. Byrne, T. Gadja, G. Hefter, S. Sjöberg, H. Wanner, "Chemical speciation of environmentally significant metals with inorganic ligands Part 2: The Cu^{2+} -OH⁻, Cl⁻, CO_3^{2-} , SO_4^{2-} , and PO_4^{3-} systems (IUPAC Technical Report)," *Pure Appl. Chem.*, vol. 79, no. 5, pp. 895–950, 2007
- [12] I. Puigdomenech and C. Taxen, "Thermodynamic data for copper. Implications for the corrosion of copper under repository conditions," INIS, Technical report TR-00-13, 2000
- [13] H.-P. Hermansson, "The Stability of Magnetite and its Significance as a Passivating Film in the Repository Environment," SKI, SKI Report 2004:07, 2004
- [14] H.-P. Hermansson, "Copper Thermodynamics in the Repository Environment up to 130°C," SRSA, Technical report 2010:09, 2010
- [15] W. Rühle, H. Neder, G. Holz, and V. Schneider, "Oxygen injection into reheating steam of moisture separator reheaters," *Power Plant Chem.*, vol. 7, no. 6, pp. 355–363, 2005
- [16] J. Riznic, *Steam Generators for Nuclear Power Plants*. Elsevier, 2017
- [17] W. Sugino, J. Fukuda, Kitano, Hisamune, Kenji, and Y. Meguro, "Effectiveness of oxygen treatment on flow accelerated corrosion mitigation on PWR secondary system," Paris, 2012
- [18] M. Ristić, B. Hannover, S. Popović, S. Musić, and N. Bajraktaraj, "Ferritization of copper ions in the Cu–Fe–O system," *Mater. Sci. Eng. B*, vol. 77, no. 1, pp. 73–82, 2000
- [19] J. Y. Kim, J. A. Rodriguez, J. C. Hanson, A. I. Frenkel, and P. L. Lee, "Reduction of CuO and Cu₂O with H₂: H Embedding and Kinetic Effects in the Formation of Suboxides," *J. Am. Chem. Soc.*, vol. 125, no. 35, pp. 10684–10692, 2003
- [20] K. C. Sabat, R. K. Paramguru, and B. K. Mishra, "Reduction of Copper Oxide by Low-Temperature Hydrogen Plasma," *Plasma Chem. Plasma Process.*, vol. 36, no. 4, pp. 1111–1124, 2016
- [21] M. Pourbaix, "Cuivre," in *Atlas d'Equilibres Electrochimiques*, vol. 14, 1963, pp. 384–392
- [22] B. Beverskog and I. Puigdomenech, "Revised Pourbaix Diagrams for Copper at 25 to 300°C," *J. Electrochem. Soc.*, vol. 144, no. 10, pp. 3476–3483, 1997
- [23] J. N. Bridson, S. E. Quinlan, and P. R. Tremaine, "Synthesis and Crystal Structure of Maricite and Sodium Iron(III) Hydroxyphosphate," *Chem. Mater.*, vol. 10, no. 3, pp. 763–768, 1998
- [24] D. Broadbent, G. G. Lewis, and E. A. M. Wetton, "The chemistry of high temperature phosphate solutions in relation to steam generation," Bournemouth, UK, 1978, pp. 53–62
- [25] S. E. Ziemniak and E. P. Opalka, "Magnetite stability in aqueous sodium phosphate solutions at elevated temperatures," in *Sixth international symposium on environmental degradation of materials in nuclear power systems : water reactors*, Knolls Atomic Power Laboratory, Schenectady, NY (United States): Gold R. E. and Simonen E. P., 1993, pp. 929–935
- [26] S. Quinlan, D. Chvedov, L. N. Trevani, and P. R. Tremaine, "Thermodynamics of the Sodium–Iron–Phosphate–Water System Under Hydrothermal Conditions: The Gibbs Energy of Formation of Sodium Iron(III) Hydroxy Phosphate, $\text{Na}_3\text{Fe}(\text{PO}_4)_2 \cdot (\text{Na}_{4/3}\text{H}_{2/3}\text{O})$, from Solubility Measurements in Equilibrium with Hematite at 498–598 K," *J. Solut. Chem.*, vol. 44, no. 5, pp. 1121–1140, 2015
- [27] P. R. Tremaine and C. Xiao, "Enthalpies of formation and heat capacity functions for maricite, $\text{NaFePO}_4(\text{cr})$, and sodium iron(III) hydroxy phosphate, $\text{Na}_3\text{Fe}(\text{PO}_4)_2 \cdot (\text{Na}_{4/3}\text{H}_{2/3}\text{O})_{(\text{cr})}$," *J. Chem. Thermodyn.*, vol. 31, no. 10, pp. 1307–1320, 1999
- [28] G. B. McGarvey and D. G. Owen, "Interactions Between Iron Oxides and Copper Oxides Under Hydrothermal Conditions," AECL EAEL, AECL-11348, 1995
- [29] D. Shishin, "Development of a thermodynamic database for copper smelting and converting," PhD Génie métallurgique, Université de Montréal, 2013
- [30] A. M. Sukhotin and K. M. Kartashova, "The passivity of iron in acid and alkaline solutions," *Corros. Sci.*, vol. 5, no. 5, pp. 393–407, 1965
- [31] P. Combrade and F. Vaillant, "Corrosion des alliages de nickel et des aciers inoxydables en milieux REP pollués ou confinés," *Tech. Ing.*, 2014
- [32] A. Stutzmann, S. Leclercq, and C. Mansour, "Chimie des milieux primaire et secondaire des centrales nucléaires REP françaises," *Tech. Ing.*, 2015